Vacuolar Transport of Abscisic Acid Glucosyl Ester Is Mediated by ATP-Binding Cassette and Proton-Antiport Mechanisms in Arabidopsis[1][W][OPEN]

Bo Burla[2,3]*, Stefanie Pfrunder[2], Réka Nagy, Rita Maria Francisco, Youngsook Lee, and Enrico Martinoia

Institute of Plant Biology, University of Zurich, 8008 Zurich, Switzerland (B.B., S.P., R.N., R.M.F., E.M.); and Pohang University of Science and Technology-University of Zurich Cooperative Laboratory, Department of Integrative Bioscience and Biotechnology, World Class University Program, Pohang University of Science and Technology, Pohang 790–784, Korea (Y.L., E.M.)

ORCID IDs: 0000-0002-5918-3249 (B.B.); 0000-0001-5561-7209 (S.P.); 0000-0002-9663-5371 (R.N.); 0000-0001-7728-8477 (R.M.F.).

Abscisic acid (ABA) is a key plant hormone involved in diverse physiological and developmental processes, including abiotic stress responses and the regulation of stomatal aperture and seed germination. Abscisic acid glucosyl ester (ABA-GE) is a hydrolyzable ABA conjugate that accumulates in the vacuole and presumably also in the endoplasmic reticulum. Deconjugation of ABA-GE by the endoplasmic reticulum and vacuolar β-glucosidases allows the rapid formation of free ABA in response to abiotic stress conditions such as dehydration and salt stress. ABA-GE further contributes to the maintenance of ABA homeostasis, as it is the major ABA catabolite exported from the cytosol. In this work, we identified that the import of ABA-GE into vacuoles isolated from Arabidopsis (*Arabidopsis thaliana*) mesophyll cells is mediated by two distinct membrane transport mechanisms: proton gradient-driven and ATP-binding cassette (ABC) transporters. Both systems have similar K_m values of approximately 1 mM. According to our estimations, this low affinity appears nevertheless to be sufficient for the continuous vacuolar sequestration of ABA-GE produced in the cytosol. We further demonstrate that two tested multispecific vacuolar ABCC-type ABC transporters from Arabidopsis exhibit ABA-GE transport activity when expressed in yeast (*Saccharomyces cerevisiae*), which also supports the involvement of ABC transporters in ABA-GE uptake. Our findings suggest that the vacuolar ABA-GE uptake is not mediated by specific, but rather by several, possibly multispecific, transporters that are involved in the general vacuolar sequestration of conjugated metabolites.

Abscisic acid (ABA) is a major plant hormone involved in various physiological and developmental processes. ABA signaling is fundamental in plant responses to abiotic stresses, including drought, cold, osmotic, and salt stress (Cutler et al., 2010). The best-characterized function of ABA is the regulation of stomatal aperture in response to environmental signals, such as soil and air humidity, temperature, and CO_2 concentration (Nilson and Assmann, 2007; Kim et al., 2010). However, ABA also has important functions in seed development, dormancy, and germination (Holdsworth et al., 2008), lateral root formation (Galvan-Ampudia and Testerink, 2011), and leaf senescence (Lim et al., 2007). Besides, ABA is not restricted only to plants; it was also identified to have functions in species from all kingdoms, including humans, and may even have universal functions (e.g. in UV-B stress response; Tossi et al., 2012).

ABA is synthesized de novo from the carotenoid zeaxanthin, whereby the first ABA-specific biosynthetic step occurs in the plastid and the final two steps take place in the cytosol (Nambara and Marion-Poll, 2005). The catabolism of ABA is mediated via oxidative and Glc conjugation pathways (Nambara and Marion-Poll, 2005). The ABA 8′-hydroxylation catalyzed by P450 cytochromes of the CYP707A subfamily represents the predominant catabolic pathway of ABA and has been demonstrated to be a key regulatory step in ABA action (Kushiro et al., 2004). The major oxidative ABA catabolites, phaseic acid (PA) and dihydroxyphaseic acid (DPA), exhibit lower and no biological activity, respectively (Sharkey and Raschke, 1980; Kepka et al., 2011). The conjugation of ABA and its oxidative catabolites PA and DPA with Glc catalyzed by UDP-glucosyltransferases represents the other mechanism of ABA inactivation. Abscisic acid glucosyl ester (ABA-GE) appears to be the major conjugate, which was found in various organs of different plant species (Piotrowska and Bajguz, 2011). In contrast to the oxidative pathway, the inactivation of ABA by Glc conjugation is reversible, and hydrolysis of ABA-GE catalyzed by β-glucosidases results in free ABA (Dietz et al., 2000; Lee et al., 2006; Xu et al., 2012). ABA-GE levels were shown to substantially increase during dehydration

[1] This work was supported by the Global Research Laboratory program of the Ministry of Science, ICT, and Future Planning of Korea (to Y.L. and E.M.) and the Swiss National Foundation (grant no. 3100AO–1177900 to E.M.).

[2] These authors contributed equally to the article.

[3] Present address: Division of Internal Medicine, University Hospital Zurich, 8091 Zurich, Switzerland.

* Address correspondence to bo.burla@uzh.ch.

The author responsible for distribution of materials integral to the findings presented in this article in accordance with the policy described in the Instructions for Authors (www.plantphysiol.org) is: Bo Burla (bo.burla@uzh.ch).

[W] The online version of this article contains Web-only data.

[OPEN] Articles can be viewed online without a subscription.

www.plantphysiol.org/cgi/doi/10.1104/pp.113.222547

and specific seed developmental and germination stages (Boyer and Zeevaart, 1982; Hocher et al., 1991; Chiwocha et al., 2003). Furthermore, ABA-GE is present in the xylem sap, where it was shown to increase under drought, salt, and osmotic stress (Sauter et al., 2002). Apoplastic ABA β-glucosidases in leaves have been suggested to mediate the release of free ABA from xylem-borne ABA-GE (Dietz et al., 2000). Therefore, ABA-GE was proposed to be a root-to-shoot signaling molecule. However, under drought stress, ABA-mediated stomatal closure occurs independently of root ABA biosynthesis (Christmann et al., 2007). Thus, the involvement of ABA-GE in root-to-shoot signaling of water stress conditions remains to be revealed (Goodger and Schachtman, 2010).

The intracellular compartmentalization of ABA and its catabolites is important for ABA homeostasis (Xu et al., 2013). Free ABA, PA, and DPA mainly occur in the extravacuolar compartments. In contrast to these oxidative ABA catabolites, ABA-GE has been reported to accumulate in vacuoles (Bray and Zeevaart, 1985; Lehmann and Glund, 1986). Since the sequestered ABA-GE can instantaneously provide ABA via a one-step hydrolysis, this conjugate and its compartmentalization may be of importance in the maintenance of ABA homeostasis. The identification of the endoplasmic reticulum (ER)-localized β-glucosidase AtBG1 that specifically hydrolyzes ABA-GE suggests that ABA-GE is also present in the ER (Lee et al., 2006). Plants lacking functional AtBG1 exhibit pronounced ABA-deficiency phenotypes, including sensitivity to dehydration, impaired stomatal closure, earlier germination, and lower ABA levels. Hydrolysis of ER-localized ABA-GE, therefore, represents an alternative pathway for the generation of free cytosolic ABA (Lee et al., 2006; Bauer et al., 2013). This finding raised the question of whether vacuolar ABA-GE also has an important function as an ABA reservoir. This hypothesis was supported by recent identifications of two vacuolar β-glucosidases that hydrolyze vacuolar ABA-GE (Wang et al., 2011; Xu et al., 2013). The vacuolar AtBG1 homolog AtBG2 forms high molecular weight complexes, which are present at low levels under normal conditions but significantly accumulate under dehydration stress. *AtBG2* knockout plants displayed a similar, although less pronounced, phenotype to *AtBG1* mutants: elevated sensitivity to drought and salt stress, while overexpression of *AtBG2* resulted in exactly the opposite effect (i.e. increased drought tolerance). The other identified vacuolar ABA-GE glucosidase, BGLU10, exhibits comparable mutant phenotypes to AtBG2 (Wang et al., 2011). This redundancy may explain the less pronounced mutant phenotypes of vacuolar ABA-GE glucosidases compared with the ER-localized AtBG1. Moreover, the fact that overexpression of the vacuolar *AtBG2* is able to phenotypically complement *AtBG1* deletion mutants indicates an important role of vacuolar ABA-GE as a pool for free ABA during the abiotic stress response (Xu et al., 2012).

The described accumulation and functions of vacuolar ABA-GE raise the question of by which mechanisms ABA-GE is sequestered into the vacuoles. To answer this question, we synthesized radiolabeled ABA-GE and characterized the ABA-GE transport into isolated mesophyll vacuoles. We showed that the vacuole comprises two distinct transport systems involved in the accumulation of ABA-GE: proton gradient-dependent and directly energized ATP-binding cassette (ABC)-type transport. In a targeted approach, we furthermore show that the Arabidopsis (*Arabidopsis thaliana*) ABC transporters AtABCC1 and AtABCC2 exhibit ABA-GE transport activity in vitro.

RESULTS

Enzymatic Synthesis of Radiolabeled ABA-GE

To analyze the transport of ABA-GE into intact plant vacuoles and yeast (*Saccharomyces cerevisiae*) membrane vesicles, we synthesized radiolabeled ABA-GE from nonlabeled ABA and [^{14}C]UDP-Glc or [^{3}H]UDP-Glc using recombinant UDP-glucosyltransferase UGT71B6 from Arabidopsis (Lim et al., 2005). The expression of recombinant UGT71B6 and the enzymatic synthesis of ABA-GE were based on a previously published method (Priest et al., 2005) and modified to obtain a high conversion efficiency of UDP-Glc into ABA-GE. We obtained approximately 25 nmol of ABA-GE from 50 nmol of UDP-Glc, corresponding to a conversion efficiency of 50% (Supplemental Fig. S1). This was sufficient for one plant vacuole or yeast vesicle uptake assay comprising up to 100 samples. UGT71B6 was shown to catalyze enantioselective glucosylation of racemic ABA in vitro, yielding up to 92% (+)-ABA-GE (Lim et al., 2005). However, the proportion of synthesized (+)-ABA-GE under our conditions is not known. To assess the purity of synthesized ABA-GE, we produced ABA-GE from nonlabeled UDP-Glc and analyzed it by HPLC. Only one major peak with an identical retention time corresponding to authentic ABA-GE was observed (Fig. 1). A minor peak corresponding to authentic ABA was also observed. The ABA contamination in the synthesized ABA-GE substrate was 1 mmol mol^{-1} or less. To further verify the identity of synthesized ABA-GE, we tested the effect of alkaline hydrolysis. After incubation with sodium hydroxide, the peak corresponding to ABA-GE completely disappeared and another peak appeared that corresponded to ABA (Fig. 1). Furthermore, both the absorption spectra of authentic and synthesized ABA-GE samples displayed absorption maxima at 270 nm (Supplemental Fig. S2).

Vacuolar ABA-GE Uptake Is Time Dependent and Enhanced by Magnesium-ATP

Isolated mesophyll vacuoles from Arabidopsis accumulated ABA-GE in a time-dependent manner (Fig. 2). The uptake was enhanced by the presence of magnesium-ATP (MgATP) and remained linear up to at least 18 min. ABA-GE is prone to hydrolysis by β-glucosidases (Dietz et al., 2000; Xu et al., 2013). β-Glucosidases, which may be

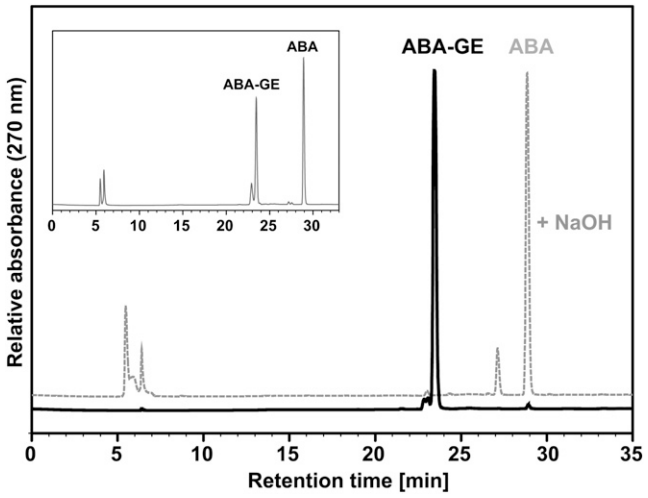

Figure 1. HPLC analysis of the synthesized and purified ABA-GE. Chromatograms show the synthesized ABA-GE before (black trace) and after (gray trace) hydrolysis with 1 M NaOH. The inset displays a chromatogram of a reference mixture containing 10 nmol of both authentic ABA-GE and ABA.

present in the vacuole preparation from lysed protoplasts and/or from disintegrated vacuoles, may hydrolyze [^{14}C]ABA-GE into [^{14}C]Glc and free ABA. Furthermore, additional enzymes such as P450 cytochromes could be present in the vacuole preparation as well, which possibly metabolize ABA-GE before it is taken up by vacuoles. Therefore, we tested the ABA-GE integrity in the reaction mix and additionally analyzed the identity of the ^{14}C-labeled compounds present in the vacuoles at the end of the uptake assays (18-min incubation time) using HPLC fractionation. In the substrate mix, 89% of the total ^{14}C radioactivity eluted in fraction 4, which corresponds to the elution time of ABA-GE (Fig. 3A). Another 8% of the radioactivity was detected in the second fraction containing the solvent front. Since free Glc is expected to elute at or near the solvent front in this HPLC setup employing a C_{18} column, we additionally analyzed the substrate mix for the presence of [^{14}C]Glc using a HPLC system for the separation of carbohydrates. The obtained fractionation profile revealed two peaks with ^{14}C radioactivity, corresponding to the elution times of Glc and ABA-GE (Supplemental Fig. S3). The [^{14}C]Glc concentration was estimated to be between 8 and 62 nM during the vacuolar uptake assay, assuming 10% hydrolysis and prevalent ABA-GE concentrations of 0.8 to 6.2 μM. In vacuole samples obtained after 18 min of incubation with the ABA-GE substrate mix, the majority of ^{14}C radioactivity was found in fraction 4, corresponding to the elution time of ABA-GE (Fig. 3B). Vacuoles incubated in the absence and presence of MgATP comprised 57% and 80% of the total radioactivity in fraction 4, respectively. Furthermore, vacuoles that were incubated in the presence of MgATP contained 2.9-fold more total ^{14}C radioactivity compared with vacuoles incubated without MgATP. In both conditions, ^{14}C radioactivity was also detected in fraction 2, corresponding to the solvent front (24% and 8% of total radioactivity, respectively). As detailed before, this radioactivity presumably corresponds to [^{14}C]Glc that originated from the hydrolysis of [^{14}C]ABA-GE.

Vacuolar ABA-GE Uptake Is Energized by Distinct Mechanisms

The presence of MgATP enhanced the ABA-GE uptake rate by an average factor of 3.3 (Fig. 4). To determine whether this enhancement is the result of a direct or indirect energization by MgATP, we tested the effects of compounds dissipating the proton gradient and inhibitors of ABC transporters in the presence of 4 mM MgATP (Fig. 4). Ammonium chloride (NH_4Cl) at 5 mM, which dissipates the proton gradient over the membrane, reduced the ABA-GE uptake activity by 28%, and 0.5 μM bafilomycin A1, a vacuolar proton pump (V-ATPase) inhibitor (Dröse and Altendorf, 1997), reduced it by 43%. Residual proton gradients present in isolated vacuoles may energize transport even when V-ATPases are inhibited. The combination of bafilomycin A1 and NH_4Cl resulted in a 58% reduction of ABA-GE uptake, which is still higher than the activity in the absence of MgATP. This indicated the existence of an additional, energized ABA-GE transport mechanism. The addition of the known ABC transporter inhibitor orthovanadate (1 mM) or glibenclamide (0.1 mM; Martinoia et al., 1993; Payen et al., 2001) likewise reduced the ABA-GE uptake activity, by 26% or 51%, respectively. Combining the inhibitors of ABC transporters and V-ATPases, orthovanadate and bafilomycin A1, resulted in 50% reduction of the ABA-GE uptake activity. While this is more than the individual effects of these compounds, it is still higher compared with the uptake activity in the absence of MgATP. To clarify whether this

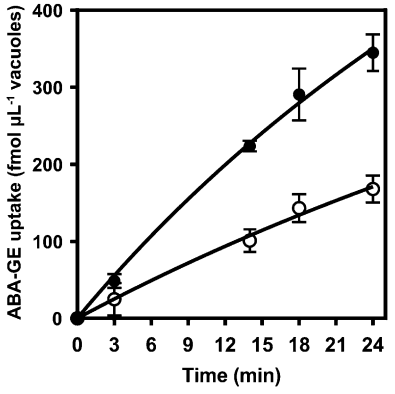

Figure 2. Time-dependent uptake of ABA-GE into isolated Arabidopsis mesophyll vacuoles in the presence (black circles) and absence (white circles) of 4 mM MgATP. The uptake was measured with an ABA-GE substrate concentration of 0.8 μM. Each data point represents the mean of five experimental replicates ± SD.

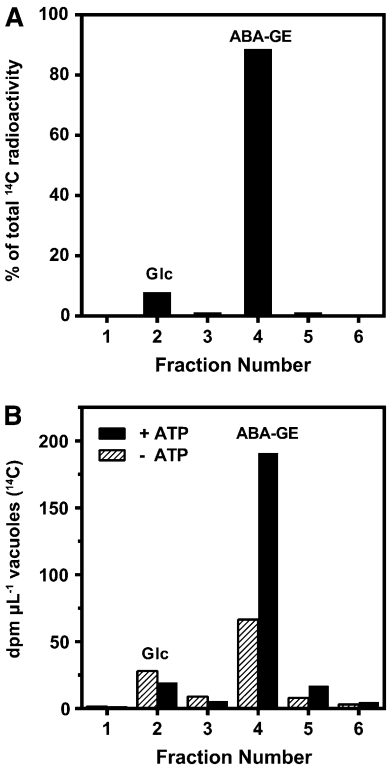

Figure 3. HPLC elution profiles of the ^{14}C radioactivity of the substrate solution (A) and of incubated vacuoles (B) after a vacuolar transport assay. Substrate solution and vacuoles were subjected to HPLC fractionation after incubation with vacuoles for 18 min in the presence (black bars) and absence (striped bars) of 4 mM ATP. Fraction 2 corresponds to the solvent front, which contained eluted Glc, and fraction 4 corresponds to the elution time of ABA-GE.

residual ABA-GE uptake activity in the absence of MgATP is the result of preexisting proton gradients present in isolated vacuoles, we tested the effect of NH_4Cl in the absence of MgATP. The addition of NH_4Cl further reduced the ABA-GE import in the absence of MgATP from 33% to 20% of the total transport activity observed in the presence of MgATP (Fig. 4). In addition, we tested the acidity in isolated vacuoles by neutral red staining. The majority of the vacuoles accumulated neutral red, indicating intact proton gradients in these vacuoles (Supplemental Fig. S4).

Specificity of the Vacuolar ABA-GE Import Mechanisms

To characterize the specificity of ABA-GE uptake, we tested compounds that potentially could compete with ABA-GE transport. The compounds were added in 40- to 2,000-fold excess of the ABA-GE concentration, which was between 0.8 and 6.2 μM in the experiments. The presence of 0.5 mM ABA, 0.1 mM UDP-Glc, 5 mM Suc, or 5 mM Glc did not significantly affect the ABA-GE uptake (Table I). Furthermore, we tested the flavonoid quercetin, which has been shown to inhibit ABC-type and proton antiporters of the multidrug and toxic compound extrusion (MATE) family (van Zanden et al., 2005; Omote et al., 2006). The presence of 0.5 mM quercetin and 0.5 mM quercetin-3-*O*-glucoside inhibited ABA-GE uptake by 71% and 60%, respectively.

Kinetics of Vacuolar ABA-GE Import

To further characterize the MgATP-activated ABA-GE uptake into mesophyll vacuoles, we analyzed the overall kinetics and the individual kinetics of the anticipated ABC-type and proton gradient-driven transport mechanisms. The individual kinetics were determined in the presence of the ABC transporter inhibitor orthovanadate (1 mM) and the V-ATPase inhibitor bafilomycin A1 (0.5 μM), respectively. All ABA-GE transport kinetics displayed Michaelis-Menten saturation curves in nonlinear regression analyses (Fig. 5) and statistically significant estimations of K_m and V_{max} ($P < 0.01$). The overall ABA-GE import exhibited an estimated K_m of 0.79 ± 0.04 mM. In the presence of bafilomycin A1, the estimated K_m was 1.24 ± 0.07 mM, and in presence of orthovanadate, the K_m was 1.02 ± 0.10 mM. The estimated V_{max} of the overall uptake was 47.5 ± 1.3 pmol μL^{-1} vacuole min^{-1} (Fig. 5A). For the individual kinetics, the estimated V_{max} in the presence of bafilomycin A1 was 6.71 ± 0.38 pmol μL^{-1} vacuole min^{-1}, and in the presence of orthovanadate, it was 13.9 ± 0.5 pmol μL^{-1} vacuole min^{-1} (Fig. 5B). Thus, the proton gradient-driven transport mechanism has a comparable affinity but an approximately

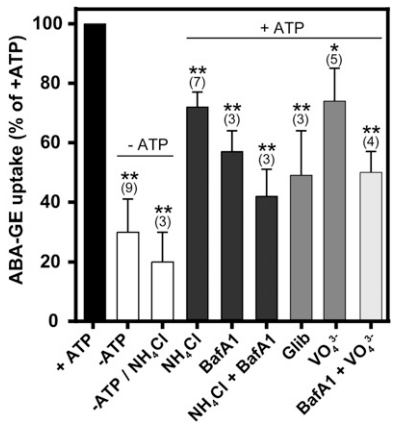

Figure 4. Effect of proton gradient modifiers and ABC transporter inhibitors on the transport of ABA-GE into isolated Arabidopsis mesophyll vacuoles. The proton gradient modifiers (dark gray bars) NH_4Cl (5 mM) and bafilomycin A1 (0.5 μM; BafA1) and the ABC transporter inhibitors (medium gray bars) glibenclamide (0.1 mM; Glib) and orthovanadate (1 mM; VO_4^{3-}) or their combination (light gray bars) were added in the presence of 4 mM MgATP. NH_4Cl at 5 mM was also tested in the absence of MgATP (white bars). ABA-GE uptake activities were determined at ABA-GE concentrations between 0.8 and 6.2 μM after incubation for 18 min. Values were normalized to the +ATP value and are given as means ± SD from n (in parentheses) independent experiments. Statistical differences versus 100% are indicated (*$P \leq 0.05$, **$P \leq 0.01$; one-sample Student's t test).

Table I. *Effect of potential competitors and inhibitors on ABA-GE import into isolated Arabidopsis mesophyll vacuoles*

ABA-GE uptake activities were determined at ABA-GE concentrations between 0.8 and 6.2 μM after incubation for 18 min. Values were normalized to the +4 mM MgATP value and are given as means ± SD from *n* independent experiments.

Assay Conditions	ABA-GE Uptake	*n*
	% of +MgATP	
−MgATP	30 ± 11	9
+4 mM MgATP	100	9
+4 mM MgATP + ABA (0.5 mM)	103 ± 9	3
+4 mM MgATP + ABA-GE (1 mM)	49 ± 9	3
+4 mM MgATP + Glc (5 mM)	103 ± 13	3
+4 mM MgATP + Suc (5 mM)	106 ± 10	3
+4 mM MgATP + UDP-Glc (0.1 mM)	114 ± 15	4
+4 mM MgATP + quercetin (0.5 mM)	29 ± 7	4
+4 mM MgATP + quercetin 3-*O*-glucoside (0.5 mM)	40 ± 11	3

2-fold higher transport activity compared with the ABC transporter-mediated mechanism.

In Vitro ABA-GE Transport Activities of Specific Arabidopsis ABCC Proteins

The Arabidopsis ABC subfamily C (ABCC) transporters AtABCC1 and AtABCC2 were previously demonstrated to localize to the vacuolar membrane (Liu et al., 2001; Geisler et al., 2004) and have been shown to transport organic anion conjugates (Lu et al., 1998; Liu et al., 2001). AtABCC14 is also localized to the tonoplast, as shown by several proteomic analyses (Carter et al., 2004; Shimaoka et al., 2004; Jaquinod et al., 2007). Besides its high and constitutive expression in all developmental stages, *AtABCC14* is substantially differentially expressed during seed maturation, imbibition, stratification, and germination (Supplemental Figs. S5 and S6). Since ABA-GE levels were reported to increase during seed maturation and germination (Chiwocha et al., 2003; Seiler et al., 2011), we hypothesized that AtABCC14 may be involved in ABA-GE transport. In a targeted approach, we tested the Arabidopsis ABCC transporters AtABCC1, AtABCC2, and AtABCC14 for their ability to transport ABA-GE using membrane vesicles isolated from yeast heterologously expressing these proteins. We obtained the yeast expression constructs pNEV-AtABCC1, pYES3-AtABCC2, and the empty vector pNEV (Song et al., 2010) and transformed them into yeast strains lacking the yeast vacuolar *ABCC* genes *yeast cadmium factor 1* (*YcF1*), *yeast bile transporter 1* (*Ybt1*), and *bile pigment transporter 1* (*Bpt1*) (Paumi et al., 2009). The full-length AtABCC14 complementary DNA (cDNA) was cloned into the yeast expression vector pNEV-N and expressed in yeast lacking Ycf1. Membrane vesicles from AtABCC14-transformed yeast did not exhibit detectable ABA-GE transport activity (Supplemental Fig. S7). In the absence of MgATP, membrane vesicles from yeast transformed with pNEV-AtABCC1 and pYES3-AtABCC2 displayed minimal ABA-GE uptake (Fig. 6A). However, in the presence of 4 mM MgATP, a distinct time-dependent ABA-GE uptake was observed, which was linear for up to 24 min (Fig. 6B). Vesicles from yeast transformed with the empty vector pNEV only displayed a minimal ABA-GE uptake, which was not enhanced by MgATP (Fig. 6). The yeast expression vectors pYES3 (Lu et al., 1997) and pNEV (Sauer and Stolz, 1994) harbor distinct constitutively expressing promoters: 3-phosphoglycerate kinase and yeast plasma membrane H^+-ATPase promoter, respectively. Therefore, the difference in uptake rates of membrane vesicles from pYES3-AtABCC2- and pNEV-AtABCC1-transformed yeast may be explained by different protein expression levels. However, AtABCC2 was previously shown to exhibit a higher transport activity for several substrates compared with AtABCC1 when expressed in the same pYES3 vector (Lu et al., 1998). To validate that MgATP-activated uptake of ABA-GE into yeast vesicles expressing AtABCC2 has the characteristics of ABC transporter-mediated transport, we tested the effects of the ABC transporter inhibitors orthovanadate and probenecid (Nagy et al., 2009) on AtABCC2-expressing yeast vesicles. The presence of 1 mM orthovanadate and 1 mM probenecid strongly inhibited the MgATP-enhanced ABA-GE uptake by 92% and 90%, respectively, which corresponds to the uptake activity in the absence of MgATP (Table II).

AtABCC1 and *AtABCC2* Transcript Levels and Knockout Phenotypes under Different Treatments

AtABCC1 and *AtABCC2* transcript abundance was approximately 2-fold increased after 8 h of incubation with 20 μM ABA, 20 μM ABA-GE, or 10 μM tetcyclacis, an ABA 8′-hydroxylase inhibitor (Kushiro et al., 2004). The combination of ABA (20 μM) with tetcyclacis (10 μM) resulted in no additional increase of *AtABCC1* transcript abundance but led to an approximately 2-fold higher *AtABCC2* expression level compared with ABA alone and a 3-fold higher level compared with the untreated control (Supplemental Fig. S8).

Additionally, we obtained *AtABCC1* and *AtABCC2* expression data from publicly available microarray

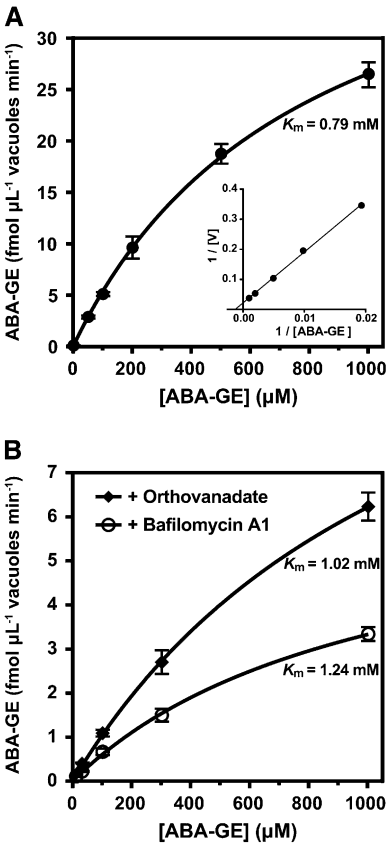

Figure 5. Effect of the ABA-GE concentration on the MgATP-dependent ABA-GE uptake of isolated Arabidopsis mesophyll vacuoles. A, ABA-GE uptake kinetics in the absence of inhibitors. The inset shows the same data represented in a Lineweaver-Burk plot. B, ABA-GE uptake kinetics in the presence of the ABC transporter inhibitor orthovanadate (1 mM; black diamonds) or the V-ATPase inhibitor bafilomycin A1 (0.5 μM; white circles). ABA-GE uptake rates were obtained by subtracting the uptake rates in the absence of MgATP from the uptake rates obtained in the presence of 4 mM MgATP. Each data point represents the mean ± SD of four experimental replicates. Apparent K_m values estimated by nonlinear regression fits are indicated. For V_{max} values, see text.

experiments via Genevestigator (www.genevestigator.com). Since we were interested in the transcriptional regulation of these transporters after the accumulation of ABA-GE, we evaluated experiments with an exposure to exogenous ABA or drought of at least 4 h (Supplemental Table S1). *AtABCC1* was not or was only minimally differently expressed under the analyzed conditions (Supplemental Fig. S9A). However, *AtABCC2* transcript levels were considerably increased after exposure to drought for at least 4 d. Treatment with exogenous ABA for 4 h resulted in only a little increase of *AtABCC2* expression (Supplemental Fig. S9B).

To test whether *atabcc1* and *atabcc2* single and *atabcc1*/*atabcc2* double mutants (Song et al., 2010) exhibited evident ABA-related phenotypes, 2-week-old seedlings were subjected to drought (polyethylene glycol [PEG]-infused plates) or osmotic (mannitol) stress for 1 week. No evident differences in wilting appearance and in root and shoot growth were observed between mutant and wild-type seedlings under the tested conditions.

DISCUSSION

ABA-GE is presumably synthesized in the cytosol via UDP-glucosyltransferases (Boursiac et al., 2013). The very low permeability of ABA-GE for biological membranes (Boyer and Zeevaart, 1982; Baier et al., 1990) implies that ABA-GE is transported across the vacuolar membrane via transporter-mediated mechanisms. Here, we demonstrate that two distinct transport mechanisms participate in the vacuolar ABA-GE sequestration, the first involves ABC-type and the second involves proton gradient-driven transporters.

To quantify the membrane transport of ABA-GE, we first established a method to efficiently synthesize

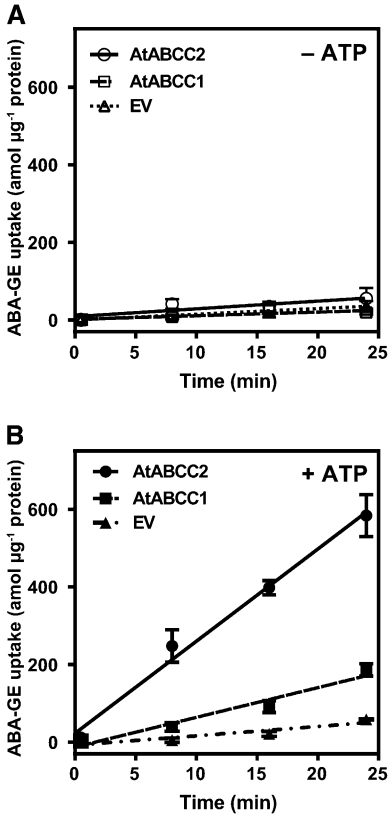

Figure 6. Time-dependent ABA-GE uptake of membrane vesicles from yeast expressing AtABCC1 and AtABCC2 in the absence (A) or presence (B) of 4 mM MgATP. Membrane vesicles were obtained from pYES3-AtABCC2 (circles), pNEV-AtABCC1 (squares), or the empty vector pNEV (EV; triangles) transformed yeast strain YMM36, which is deleted in the yeast *ABCC* genes *Ycf1*, *Ybt1*, and *Bpt1*. ABA-GE uptake was determined at an ABA-GE concentration of 40 nM. Each data point represents the mean ± SD of three experimental replicates from one representative experiment out of three experiments with independent vesicle preparations.

Table II. *Effect of MgATP and of ABC transporter inhibitors on the ABA-GE uptake of membrane vesicles isolated from pYES3-AtABCC2-transformed yeast*

Yeast membrane vesicles were preincubated with inhibitors, and uptake activities were determined for each condition once at an ABA-GE concentration of 1.4 μM, whereas the remaining experiments were tested at 34 to 70 nM ABA-GE. Values were normalized to the +4 mM MgATP value and are given as means ± SD from *n* independent experiments.

Assay Conditions	ABA-GE Uptake	*n*
	% of +MgATP	
−MgATP	15 ± 8	6
+4 mM MgATP	100	6
+4 mM MgATP + orthovanadate (1 mM)	8 ± 3	3
+4 mM MgATP + probenecid (1 mM)	10 ± 12	3

radiolabeled ABA-GE in high purity from commercially available [^{3}H]UDP-Glc and [^{14}C]UDP-Glc (Fig. 1). Using this method, radiolabeled ABA-GE sufficient for one assay with up to 100 conditions and replicates could be synthesized from a single enzymatic reaction and subsequent HPLC-based purification. Nevertheless, the costs for radiolabeled [^{14}C]UDP-Glc imposed restrictions on the dimension and number of experiments. Intact vacuoles isolated from Arabidopsis leaf mesophyll protoplasts exhibited a time-dependent ABA-GE uptake that was enhanced by MgATP, indicating that ABA-GE transport is energized (Fig. 2). This energized transport is mediated by at least two distinct transport mechanisms (Fig. 4). The partial inhibition of the MgATP-dependent ABA-GE uptake by compounds that alter the proton gradient (NH_4Cl, which dissipates the proton gradient, and bafilomycin A1, a vacuolar H^+-ATPase inhibitor; Dröse and Altendorf, 1997) over the tonoplast indicates that proton-dependent antiport mechanisms are involved in ABA-GE transport. Likewise, the reduction of the MgATP-dependent ABA-GE uptake in the presence of inhibitors of ABC transporters (orthovanadate and glibenclamide) reveals that an ABC-type transport mechanism represents the other component of vacuolar ABA-GE uptake. The simultaneous addition of ABC transporter and V-ATPase inhibitors inhibited the ABA-GE uptake below the levels observed for these compounds individually. Orthovanadate and bafilomycin A1 were used at concentrations shown to completely inhibit corresponding enzymatic activity in tonoplast preparations (Frelet-Barrand et al., 2008; Zhao and Dixon, 2009). The presence of the preexisting proton gradients in isolated vacuoles explains why the combination of bafilomycin A1 with NH_4Cl decreased the ABA-GE uptake more than bafilomycin A1 alone. This is supported by the observed neutral red accumulation of isolated vacuoles (Supplemental Fig. S4) and by the fact that the addition of NH_4Cl reduced ABA-GE uptake also in the absence of MgATP. Therefore, residual ABA-GE uptake determined in the presence of both ABC and V-ATPase inhibitors, or in absence of MgATP, may be the result of proton antiporters driven by the prevailing proton gradient present in isolated vacuoles. Taken together, our data reveal that ABA-GE uptake into isolated mesophyll vacuoles is essentially mediated by energized transport processes, consisting of proton-dependent and ABC-type transport systems.

During vacuolar ABA-GE uptake assays, 10% of the radiolabeled [^{14}C]ABA-GE decayed in the incubation medium (Fig. 3A). Our HPLC analyses demonstrated that in the presence of MgATP, approximately 90% of the ^{14}C radioactivity measured in the vacuoles corresponded to [^{14}C]ABA-GE (Fig. 3B). The residual 10% radioactivity represents [^{14}C]Glc, which may have derived from the intravacuolar hydrolysis of imported [^{14}C]ABA-GE and/or from the vacuolar uptake of free [^{14}C]Glc present in the incubation medium. The vacuolar [^{14}C]Glc concentration appeared to be independent of the proton gradient and of the [^{14}C]ABA-GE concentration in the vacuoles, suggesting a passive import of [^{14}C]Glc from the incubation medium. Facilitated diffusion was shown to be the predominant vacuolar uptake mechanism for Glc in barley (*Hordeum vulgare*; Martinoia et al., 1987). Since the vacuoles only contained a small amount of [^{14}C]Glc, we conclude that the observed [^{14}C]Glc uptake had only a little effect on the measured ABA-GE uptake activities.

The overall MgATP-dependent ABA-GE uptake had a K_m of 0.8 mM, whereas the individual ABC-type and proton gradient-driven transporter systems had apparent K_m values of 1.0 and 1.2 mM, respectively (Fig. 5). The V_{max} of the proton-driven ABA-GE uptake was about 2-fold higher compared with the ABC transporter-mediated ABA-GE uptake; thus, the proton-dependent antiport mechanism may transport ABA-GE at an approximately 2-fold higher rate at any given ABA-GE concentration. This rather high K_m was not expected for the transport of a compound that is present at supposedly low concentrations. Consequently, the question was raised whether a transport system with these kinetic properties would be capable of sequestering cytosolic ABA-GE into the vacuole under in vivo conditions. Therefore, we made an estimation of the ABA-GE transport conditions using both data from Bray and Zeevaart (1985), who described the subcellular compartmentalization of ABA-GE in *Vicia faba* mesophyll cells, and our measured vacuolar ABA-GE transport rates (Supplemental Data S1). According to our estimations, the ABA-GE concentration in the vacuole is 117 nM and that in the cytosol is 47 nM. This estimated cytosolic ABA-GE concentration is considerably lower than the apparent K_m of 0.8 mM of the ABA-GE transport systems characterized here. Nevertheless, our calculations suggest that the estimated vacuolar ABA-GE accumulation would be reached within 2 h at the assumed constant cytosolic ABA-GE concentration. Moreover, ABA-GE levels in leaves were shown to be relatively constant and only to substantially increase during repeated drought stress cycles (Boyer and Zeevaart, 1982). Hence, despite the low affinity for ABA-GE, the identified vacuolar ABA-GE import mechanisms are possibly

adequate for the maintenance of vacuolar ABA-GE levels in vivo under normal conditions and presumably also can accommodate increasing cytosolic ABA-GE levels that occur (e.g. during drought stress conditions).

The energized transport of glucosides of secondary metabolites and xenobiotics into plant vacuoles is well documented. The anthocyanin malvidin-3-*O*-glucoside is transported into vacuoles of grape (*Vitis vinifera*) berries by the ABCC transporter ABCC1 from grape (Francisco et al., 2013). Proton gradient-dependent vacuolar transport mechanisms were reported for diverse flavonoid glucosides (Klein et al., 1996; Frangne et al., 2002; Zhao and Dixon, 2009; Zhao et al., 2011). Moreover, the vacuolar import mechanism of particular Glc conjugates was found to be species or tissue specific. Salicylic acid glucoside is transported into vacuoles from tobacco (*Nicotiana tabacum*) culture cells by proton-dependent transport mechanisms and into vacuoles from soybean (*Glycine max*) hypocotyls by ABC-type transport mechanisms (Dean and Mills, 2004; Dean et al., 2005). The glucoside of coniferyl alcohol was shown to be transported into endomembrane-enriched vesicles isolated from differentiating xylem of poplar (*Populus* spp.) via proton antiporters and into Arabidopsis leaf mesophyll vacuoles via ABC transporters (Miao and Liu, 2010; Tsuyama et al., 2013). Furthermore, concurrent ABC-type and proton-dependent vacuolar transport mechanisms were shown for the flavone diglucoside saponarin (Frangne et al., 2002). Hence, our findings on the simultaneous transport of ABA-GE by proton-dependent and ABC-type mechanisms are in agreement with previous reports on the vacuolar import of glucosides. The reported K_m values of these vacuolar transports were in range of 10 to 100 μM, which is 10- to 100-fold lower than the apparent K_m of the ABA-GE import. On the other hand, the V_{max} of the ABA-GE uptake was higher compared with some reported glucoside transports, such as that of saponarin (Frangne et al., 2002).

The vacuolar membrane localization of Arabidopsis ABCC-type transporters and the recent demonstration that grape ABCC1 mediates the vacuolar transport of anthocyanidin glucosides (Kang et al., 2011; Francisco et al., 2013) suggested the participation of ABCC-type transporters in vacuolar ABA-GE accumulation. The Arabidopsis AtABCC1 and especially AtABCC2 mediate the transport of structurally diverse metabolites, such as phytochelatins, folates, and conjugates of chlorophyll catabolite and xenobiotics (Liu et al., 2001; Frelet-Barrand et al., 2008; Raichaudhuri et al., 2009; Song et al., 2010). We expressed AtABCC2 in yeast and observed a distinct MgATP-dependent ABA-GE transport activity of isolated membrane vesicles (Fig. 6). This transport was nearly fully abolished in the presence of ABC transporter inhibitors (Table II). We furthermore tested AtABCC1, the closest paralog of AtABCC2. It also mediated MgATP-dependent ABA-GE transport in yeast membrane vesicles, indicating that a subset of ABCCs can mediate ABA-GE transport. In contrast, AtABCC14 did not exhibit ABA-GE transport activity in our analyses (Supplemental Fig. S7). Under standard growth conditions, *AtABCC1* and *AtABCC2* single and double knockout mutants exhibit no mutant phenotypes (Raichaudhuri et al., 2009; Park et al., 2012). We also did not observe growth phenotypes of these mutant seedlings subjected to drought and osmotic stress. Possible explanations are that ABA is predominantly catabolized via the oxidative pathway to PA and DPA (Huang et al., 2008; Okamoto et al., 2011) or that additional vacuolar ABA-GE transporters are present. However, in our real-time PCR analyses, *AtABCC1* and *AtABCC2* expression levels were higher after exposure to exogenous ABA and ABA-GE and to tetcyclacis, an inhibitor of P450 cytochromes (Rademacher, 2000). *AtABCC2* transcript levels were further enhanced when tetcyclacis and ABA were combined, which may result from higher levels of ABA-GE and/or reduced ABA catabolism due to the absence of cytochrome CYP707A ABA hydroxylase activity (Okamoto et al., 2011). Nevertheless, it should be kept in mind that tetcyclacis also inhibits other P450 cytochromes, which in turn may also alter *AtABCC1* and *AtABCC2* transcript levels (Rademacher, 2000). Additionally, *AtABCC2* transcript levels were reported to be increased upon exposure to drought stress in publicly available microarray data sets. Taken together, these data suggest that ABA-GE transport mediated by AtABCC1 and AtABCC2 is enhanced under conditions where ABA and ABA-GE levels are increased, albeit their contribution to the overall vacuolar ABA-GE import remains to be determined.

Members of the MATE transporter superfamily have been shown to mediate the proton-dependent vacuolar sequestration of flavonoid glucosides (Marinova et al., 2007; Zhao and Dixon, 2009; Zhao et al., 2011). In Arabidopsis, the MATE superfamily consists of 56 members (The Arabidopsis Genome Initiative, 2000). It is conceivable, therefore, that particular members of the MATE family constitute the components of the identified proton gradient-dependent mechanism involved in ABA-GE transport. Several MATE and ABCC-type proteins implicated in vacuolar conjugate transport have been shown to be multispecific (i.e. they transport structurally unrelated compounds, whereby the affinities toward the individual substrates vary considerably; Liu et al., 2001; Martinoia et al., 2012). The low affinity of the ABA-GE transport further suggests that multispecific transporters involved in the vacuolar sequestration of different metabolites also mediate the uptake of ABA-GE.

In conclusion, we show that two differently energized transporter systems mediate the import of ABA-GE into isolated mesophyll vacuoles of Arabidopsis. These systems consist of proton gradient-dependent and ABC-type transporters and exhibit similar K_m values that are largely above the reported cytosolic ABA-GE concentration. This active transport of ABA-GE, despite its low activity, appears to be sufficient in providing a constant vacuolar ABA-GE pool that allows the rapid generation of free ABA under stress conditions. The role of this transport in ABA catabolism and thus also in the

regulation of cytosolic ABA levels, however, has yet to be elucidated. The participation of two different import mechanisms and their low affinities suggest a nonspecific vacuolar transport of ABA-GE. The ABC-type transport system for ABA-GE possibly includes ABCC-type transporters that have been implicated in the vacuolar sequestration of conjugates of structurally diverse compounds. Therefore, we conclude that the vacuolar ABA-GE accumulation is not the result of specific, but rather the result of several, possibly multispecific, transporters, which are involved in the general vacuolar sequestration of conjugated metabolites and which mediate a constitutive vacuolar import of ABA-GE.

MATERIALS AND METHODS

Plant Material and Growth Conditions

Wild-type Arabidopsis (*Arabidopsis thaliana*) plants of the Columbia-0 accession were grown on standardized soil (ED73; Einheitserde Werkverband; www.einheitserde.de) in a controlled growth chamber at 20°C ± 2°C and 60% ± 10% relative humidity under short-day conditions (8 h of light and 16 h of dark) with a light intensity of 80 to 120 μmol m^{-2} s^{-1}. One week prior to the vacuole isolation, the light intensity was reduced to 50 μmol m^{-2} s^{-1}. For testing mutant phenotypes and for *AtABCC1*/*AtABCC2* expression analyses, wild-type and mutant Arabidopsis seeds were surface sterilized for 5 min in 70% (v/v) ethanol followed by 10 min in 30 g L^{-1} sodium hypochlorite supplemented with 5 g L^{-1} Tween 20, rinsed five times with water, and stratified for 4 d at 4°C in darkness. Seeds were germinated on plates containing one-half-strength Murashige and Skoog mix (1/2MS; modification 1B; Duchefa), pH 5.7, 10 g L^{-1} Suc, and 8.5 g L^{-1} phytoagar (Duchefa) in a growth chamber with 21°C and a light intensity of 90 to 130 μmol m^{-2} s^{-1} in cycles of 16 h of light and 8 h of dark. *AtABCC1* and *AtABCC2* single and double knockout mutants (all in the Columbia-0 background) were provided by Dr. Won-Yong Song (Song et al., 2010).

Expression of the Recombinant UDP-Glucosyltransferase AtUGT71B6

The expression and purification of the recombinant ABA UDP-glucosyltransferase AtUGT71B6 (Lim et al., 2005) was performed with the GST Gene Fusion System (GE Healthcare) with modifications. The intron-free *AtUGT71B6* gene was directly amplified from Arabidopsis genomic DNA with the primers 5′-CCGGAATTCATGAAAATAGAGCTAGTATTCATTCCCTC-3′ and 5′-CCCGCTCGAGCTAGCTTTCAGTTTCCGACCAA-3′ and ligated into the glutathione *S*-transferase gene fusion vector pGEX-4T-1 using the *Bam*HI/*Xho*I restriction sites. The resulting plasmid was transformed into the *Escherichia coli* BL21-CodonPlus(DE3)-RIL strain (Agilent Technologies). An overnight preculture from a fresh transformant colony was grown in 20 mL of Luria-Bertani medium containing 100 μg mL^{-1} ampicillin. A 4-mL aliquot of this preculture was inoculated in 400 mL of prewarmed 2× yeast extract tryptone medium (16 g L^{-1} tryptone, 10 g L^{-1} yeast extract, 5 g L^{-1} NaCl, adjusted to pH 7.0 with NaOH) containing 100 μg mL^{-1} ampicillin and grown at 30°C with vigorous shaking to an optical density at 600 nm of 1.0 to 1.2. This culture was then cooled on ice to approximately 14°C to 18°C, and isopropylthio-β-galactoside was added at a final concentration of 0.4 mM. After incubation at 14°C for 16 h, cells were harvested by centrifugation at 7,700*g* for 10 min at 4°C, resuspended in 20 mL of ice-cold 1× phosphate-buffered saline containing 1% (w/v) Triton X-100, and frozen overnight at −20°C. The following day, the suspension was thawed on ice, briefly sonicated with five bursts of 3 s, and centrifuged at 12,000*g* for 10 min at 4°C. The supernatant was incubated with 400 μL of a 50% slurry of Glutathione Sepharose 4B beads (GE Healthcare Life Sciences) for 30 min at room temperature. After washing three times with ice-cold 1× phosphate-buffered saline, fusion proteins were eluted three times with 200 μL of 20 mM reduced glutathione and 120 mM NaCl in 100 mM Tris-HCl, pH 8.0, for 10 min at room temperature. Pooled eluates were concentrated with a 30-kD Amicon Ultra 0.5-mL centrifugation ultrafilter (Millipore) to a protein concentration greater than 5 μg μL^{-1}, determined with the Bradford protein assay (Bio-Rad) using bovine serum albumin (BSA) as the standard. After adding glycerol to a final concentration of 10% (w/v), the enzyme solution was aliquoted and stored at −80°C.

Enzymatic Synthesis of Radiolabeled ABA-GE

Radiolabeled ABA-GE was enzymatically synthesized using the recombinant ABA glucosyltransferase AtUGT71B6 with ABA and ^{3}H- or ^{14}C-labeled UDP-Glc as substrate. UDP-[6-^{3}H]Glc was obtained from Perkin-Elmer. UDP-[U-^{14}C]Glc was first obtained from American Radiolabeled Chemicals and then from Perkin-Elmer. To verify the quality of stored [^{3}H]UDP-Glc and [^{14}C]UDP-Glc, we assessed the chemical and radiochemical purity using an ion-pairing HPLC method published by Lazarowski et al. (2003). The enzymatic synthesis of ABA-GE was based on a previously described protocol (Priest et al., 2005). The reaction was performed in a final volume of 100 μL, containing 10 to 40 nmol of [^{14}C]UDP-Glc or 0.9 nmol of [^{3}H]UDP-Glc (evaporated to dryness using a SpeedVac at room temperature), 5 mM (±)-ABA (Sigma; 50 mM stock solution; prepared by suspending in water and adding KOH until fully dissolved, pH 7.0 to 8.0, stored at –20°C), 10 mM dithiothreitol (DTT), 5 mM $MgCl_2$, and 5 to 7 μg of recombinant UGT71B6 enzyme in 100 mM Tris-HCl, pH 7.0. After incubation for 12 h at 30°C, the reaction was stopped by the addition of 20 μL of TCA (240 mg mL^{-1}) and centrifugation at 12,000*g* for 5 min at 4°C. The supernatant was immediately used for HPLC purification of the synthesized ABA-GE. The analytical reverse-phase HPLC system consisted of a Hypersil C18 ODS-2 column (5 μm, 250 × 4.6 mm; Thermo Scientific) and a 30-min linear gradient of 10% to 80% methanol in 0.1 M acetic acid, pH 3.5 (adjusted with triethylamine), at a flow rate of 0.5 mL min^{-1}. The UV absorbance of ABA-GE and ABA was monitored at a wavelength of 270 nm with a photodiode array detector (Dionex PDA-100). Authentic (±)-cis,trans-ABA-GE (OlChemIM) and (±)-ABA were used as reference compounds. The mobile phase containing the eluted peak corresponding to ABA-GE was collected into a glass vial and evaporated to dryness under a N_2 stream at approximately 50°C. Finally, the tube was filled with argon, sealed, and stored at −20°C with desiccant up to 3 months. To verify the purity and identity of the ABA-GE synthesized with this method, four enzymatic ABA-GE synthesis reactions with 30 nmol of nonradiolabeled UDP-Glc (Sigma) were performed. The purifications were conducted as described, and the obtained dried ABA-GEs were redissolved in 100 μL of water and pooled. Aliquots of 100 μL were mixed with 11 μL of water or 10 N NaOH. Following incubation for 1 h at 30°C, 100 μL of each mix was injected into the previously described HPLC system, which was used for the purification.

Isolation of Arabidopsis Mesophyll Vacuoles

The preparation of intact Arabidopsis mesophyll vacuoles was based on previously described procedures (Frangne et al., 2002; Song et al., 2003), which were further optimized. All experimental steps were performed on ice, and all centrifugations were carried out without break, unless otherwise stated. BSA and DTT were always added before use as 100× stock solutions in water. The abaxial epidermises of leaves from 6- to 8-week-old plants (see above) were abraded with P500 sandpaper, and the leaves were immediately floated on mesophyll buffer (500 mM sorbitol, 1 mM $CaCl_2$, and 10 mM MES-KOH, pH 5.6) supplemented with 1 mg mL^{-1} BSA in petri dishes. Subsequently, the leaves were incubated for 2 h at 30°C with their abaxial side on mesophyll buffer containing 10 mg mL^{-1} cellulase R10 and 5 mg mL^{-1} macerozyme R10 (Serva Electrophoresis). The suspensions with released protoplasts were collected into 50-mL Falcon tubes, each of which was underlaid with 2 mL of Percoll, pH 6 (500 mM sorbitol, 1 mM $CaCl_2$, and 20 mM MES in 100% Percoll; GE Healthcare). After centrifugation at 400*g* for 8 min at 4°C, the supernatant was aspired and the concentrated protoplasts were resuspended in the remaining solution. Additional Percoll, pH 6, was then added to a final Percoll concentration of 40%. Protoplasts were further purified by applying the following step gradient: 1 volume of protoplast suspension was overlaid with 1 volume of a 3:7 (v/v) mix of Percoll, pH 7.2 (500 mM sorbitol and 20 mM HEPES in 100% Percoll) and sorbitol buffer (400 mM sorbitol, 30 mM potassium gluconate, and 20 mM HEPES, pH 7.2, adjusted with imidazole) and then with 0.7 volume of sorbitol buffer containing 1 mg mL^{-1} BSA and 1 mM DTT. Following centrifugation at 250*g* for 8 min at 4°C, purified protoplasts were collected from the interface between the middle and upper phases into new 50-mL Falcon tubes and mixed with an equal volume of 42°C prewarmed lysis buffer (200 mM sorbitol, 20 mM EDTA, 10 mM HEPES, pH 8.0, with KOH, 10% Ficoll [GE Healthcare], 0.2 mg mL^{-1} BSA, and 1 mM DTT) and incubated at room temperature under gentle mixing by inversion of the tube. Progression of the vacuole release was monitored every 2 min by light microscopy. The reaction was stopped when most protoplasts were lysed

or at the latest after 10 min by immediate cooling of the lysates on ice and distribution into ice-cold glass centrifugation tubes. The vacuoles were purified and concentrated with the following step gradient: 1 volume of lysate was overlaid with 1 volume of a 1:1 (v/v) mixture of lysis buffer and betaine buffer (400 mM betaine, 30 mM potassium gluconate, 20 mM HEPES, pH 7.2, adjusted with imidazole, 1 mg mL^{-1} BSA, and 1 mM DTT) and then 0.2 volume of betaine buffer. After centrifugation at 1,300*g* for 8 min at 4°C, purified vacuoles were collected from the interface between the middle and upper layers and transferred to a microcentrifuge tube. The purity and density of the vacuole suspension were inspected using phase-contrast microscopy. Immediately before use, vacuoles were supplemented with Percoll, pH 7.2, to a final concentration of 32% Percoll.

Vacuolar ABA-GE Transport Assays

The [^{14}C]ABA-GE import into isolated vacuoles was determined using the silicon oil centrifugation technique (Martinoia et al., 1993). The substrate mix contained 0.8 to 6.2 μM [^{14}C]ABA-GE, 47% (v/v) 100% Percoll, pH 7.2 (see above), 2.8 mg mL^{-1} BSA, 1.4 mM DTT, 0.1 μCi of ^3H_2O, and, for –ATP reactions, 1.42 mM $MgCl_2$/48% (v/v) sorbitol buffer (see above) or, for +ATP reactions, 7.15 mM $MgCl_2$/5.7 mM ATP (diluted from a stock of 0.2 M ATP disodium salt in 0.2 M Bis-Tris propane)/42% (v/v) sorbitol buffer. Reactions were performed in 0.4-mL polyethylene microcentrifuge tubes containing 70 μL of the corresponding substrate mix. The uptake reaction was started by adding 30 μL of vacuole suspension. Subsequently, the mix was overlaid with 200 μL of silicone oil AR200 (Sigma-Aldrich) and then with 60 μL of water. After incubation at room temperature, reactions were terminated by flotation of the vacuoles through the silicon oil layer by centrifugation at 10,000*g* for 20 s. A total of 50 μL of the upper aqueous phase was mixed with 3 mL of Ultima Gold (Perkin-Elmer) scintillation cocktail, and the ^{3}H and ^{14}C radioactivity was determined by liquid scintillation counting. Each condition and time point was tested with four to five replicates. The net ABA-GE uptake values were calculated by subtracting the total uptake values with the level of nonspecifically bound ABA-GE at 0 min, which was estimated by extrapolating the 3- and 18-min uptake levels. The ABA-GE uptake values were finally normalized to the vacuolar volume per reaction by using the ^{3}H counts from ^3H_2O. Potential uptake inhibitors were tested by adding 1 μL of one of the following stock solutions to 70 μL of uptake mix: 100 mM sodium orthovanadate (dissolved in water and boiled 5 min at 95°C immediately before use), 500 mM NH_4Cl (dissolved in water), 10 mM glibenclamide (Sigma; dissolved in dimethyl sulfoxide [DMSO]), 50 μM bafilomycin A1 (Wako Pure Chemicals; dissolved in ethanol), 10 mM UDP-Glc (Sigma; in water), 500 mM Glc (in water), 500 mM Suc (in water), 50 mM quercetin or 50 mM quercetin 3-*O*-glucopyranoside (both from Extrasynthèse; dissolved in DMSO), 50 mM ABA (see "Enzymatic Synthesis of Radiolabeled ABA-GE"), or 0.5 μL of 20 mM (±)-cis, trans-ABA-GE (OlChemIM; in ethanol). For the determination of kinetic parameters, corresponding amounts of the 20 mM ABA-GE stock solution in ethanol were evaporated under a N_2 stream and redissolved with the corresponding transport mix containing [^{14}C]ABA-GE. Independent experiments represent distinct vacuole isolations followed by independent transport assays. The Michaelis-Menten nonlinear least-square regression fits were calculated using the SSmicmen function without initial parameters within the nls function of R 2.14.0 (www.R-project.org).

HPLC Analysis of Vacuoles and the Substrate Mix

To analyze the stability of [^{14}C]ABA-GE in the uptake mix during incubation with vacuoles, the substrate mixes from three uptake reactions were collected and pooled after they had been incubated with vacuoles for 18 min and centrifuged. To examine the source of ^{14}C radioactivity accumulated in vacuoles, the upper aqueous phases of five uptake reactions were pooled. Each of these samples was mixed with 0.2 volume of 240 mg mL^{-1} TCA and centrifuged at 12,000*g* for 5 min at 4°C. Subsequently, 5 μL of the substrate mix samples (diluted with 95 μL of water) and 100 μL of the vacuole samples were injected into the HPLC system used for the ABA-GE purification (see above). Fractions were collected every 3 min, concentrated to approximately 50 μL in a SpeedVac at 30°C, mixed with 3 mL of Ultima Gold scintillation cocktail (Perkin-Elmer), and measured by liquid scintillation counting. Additionally, 10 μL of the substrate mix was analyzed for the presence of [^{14}C]Glc by HPLC fractionation and subsequent liquid scintillation of 1-min fractions using the chromatographic system described by Peters et al. (2007).

Yeast Strains and Expression Constructs

The yeast (*Saccharomyces cerevisiae*) expression constructs pNEV-AtABCC1 and pYES3-AtABCC2 (Song et al., 2010) and the empty vector pNEV-N (Sauer and Stolz, 1994) were transformed by electroporation into the yeast mutant strain *YMM36* (*MATa Δyll015::HIS3-MX6 Δyll048::TRP1-MX6 Δycf1::HIS3-MX6*; courtesy of Prof. Karl Kuchler), which is a derivative of YPH499 and YPH500 (Sikorski and Hieter, 1989). Transformants were selected on minimal synthetic dropout medium without uracil. *AtABCC14* was cloned into pNEV (Sauer and Stolz, 1994) via homologous recombination. Its full-length cDNA was amplified from Arabidopsis adult rosette leaf total RNA using the High Fidelity PCR Extender Polymerase mix (5 PRIME) with the primers AtABCC14-f (5′-TTATACACACATTCAAAAGAAAGAAAAAAAATATACCCCAGCCGCGGCCGCGTACAAAAAAGCAGGCTATGCGGTGGCTTTCTTCTACG-3′) and AtABCC14-r (5′-TAAGGTGTGTGTGTGGATAAAATATTAGAATGACAATTCCGCGGCGGCCGCTACAAGAAAGCTGGGTTATTCCGGCAGATCGGAGAGC-3′). The amplified *AtABCC14* and *Not*I-linearized pNEV were cotransformed into the yeast mutant strain *ybt1* (*MATa; ura3Δ::HIS3; leu2-3, 112; his3-Δ200; bat1Δ1::URA3*; Giaever et al., 2002) by electroporation. Transformants were selected on synthetic dropout medium without uracil, and the obtained pNEV-AtABCC14 construct was recovered and verified by sequencing.

Preparation of Yeast Total Membrane Microsomes

Yeast microsomes were prepared as described by Tommasini et al. (1996). The total protein concentration in microsomal extract was quantified using the Bradford assay (Bio-Rad; with BSA as a standard). The intactness of the microsomal preparations was assessed using the 9-amino-6-chloro-2-methoxyacridine dye fluorescence quenching method described by Gomez et al. (2009).

Yeast Microsomal ABA-GE Transport Assays

The determination of radiolabeled ABA-GE import into microsomal vesicles was based on the previously described rapid filtration technique (Tommasini et al., 1996). The reaction mix for microsomal uptake assays contained 1.4 μM [^{14}C]ABA-GE or 40 to 70 nM [^{3}H]ABA-GE, 10 mM Tris-HCl, pH 7.4, 250 mM Suc, 10 mM creatine phosphate disodium salt, 100 μg mL^{-1} creatine phosphokinase from rabbit muscle (Sigma), and, for –ATP reactions, 1 mM $MgCl_2$ or, for +ATP reactions, 10 mM $MgCl_2$ and 4 mM ATP (diluted from a stock of 0.2 M Na_2ATP in 0.2 M Bis-Tris propane). A 0.15-volume microsome suspension, previously thawed on ice, was added to initiate the uptake reaction. After incubation at room temperature, the reaction (replicate) was terminated by transferring 100 μL of the mix into 950 μL of ice-cold wash buffer (0.4 M glycerol, 0.1 M KCl, and 20 mM Tris-MES, pH 7.4). Immediately after a replicate series (n = 3), 950 μL of each stopped reaction was filtered through a HA 0.45-μm nitrocellulose filter (25-mm diameter; Millipore) and washed three times with 2 mL of ice-cold wash buffer. Filters were air dried and mixed with 3 mL of Ultima Gold scintillation cocktail (Perkin-Elmer) in scintillation counter tubes, which were vigorously shaken and measured in a scintillation counter. Uptake determinations in the presence of the ABC transporter inhibitors orthovanadate and probenecid were performed by preincubating the yeast microsomes in the reaction mix containing 1 mM sodium orthovanadate (added from a fresh 100 mM stock solution in water that was boiled 5 min at 95°C before use) or 1 mM probenecid (Sigma; diluted from a 100 mM stock solution in DMSO), respectively, in the absence of ABA-GE for 10 min at room temperature. Subsequently, radiolabeled ABA-GE was added to the mix, and the experiment was continued as described above. Microsomal ABA-GE uptake was normalized with the total protein concentration of the microsomes. Experiments were repeated three times with microsomes from independent batches unless stated otherwise.

Mutant Phenotype Analyses of *AtABCC1* and *AtABCC2* Knockout Plants

Mutant phenotypes were tested by transferring 2-week-old wild-type and *atabcc1* and *atabcc2* single and *atabcc1/atabcc2* double mutant seedlings grown on plates onto plates (see "Plant Material and Growth Conditions") containing 1/2MS medium (pH 5.7) and 8.5 g L^{-1} phytoagar supplemented with 150, 300, or 500 mM mannitol or infused with 400 or 700 g L^{-1} PEG-8000. The PEG-infused plates were prepared according to a protocol by Verslues et al. (2006) and had estimated final water potentials of −0.7 and −1.7 MPa. The growth and appearance of seedlings were visually inspected from high-resolution photographs captured daily with a flatbed scanner.

Quantitative Real-Time PCR for *AtABCC1* and *AtABCC2*

Three-week-old wild-type Arabidopsis seedlings grown on plates were transferred onto plates containing 1/2MS medium (pH 5.7) and 8.5 g L^{-1} phytoagar supplemented with 20 μM ABA, 20 μM ABA-GE, 10 μM tetcyclacis, and 20 μM ABA + 10 μM tetcyclacis. ABA and ABA-GE were diluted from stock solutions described in "Vacuolar ABA-GE Transport Assays." Tetcyclacis (courtesy of Prof. Wolfram Hartung, University Würzburg) was diluted from a 50 mM stock solution in DMSO. Seedlings were incubated for 8 h under light in the same chamber used for seedling growth. Total RNA was then extracted from three pooled shoots excised from three seedlings in triplicate, using the Promega SV total RNA isolation kit with on-column DNase treatment following the manufacturer's instructions. Total RNA (1 μg) was reverse transcribed using Moloney murine leukemia virus (H−) reverse transcriptase (Promega) and oligo$(dT)_{15}$ primer in a final volume of 20 μL. Quantitative real-time PCR was performed on an Applied Biosystems 7500 Fast Real-Time PCR system with software version 2.0.4. PCR was performed in triplicate and contained 5 μL of 1:10 (v/v) diluted cDNA (corresponding to 20 ng of reverse transcribed mRNA), 10 μL of SYBR Green PCR Master Mix (Applied Biosystems), and 0.25 μM of each primer in a final volume of 20 μL. The PCR program consisted of an initial 10 min at 95°C followed by 40 cycles of 15 s at 95°C and 1 min at 60°C. The following intron-spanning primer pairs were used: *AtABCC1*-forward, 5′-TATTACCAGAACACATCTCGGGA-3′, and *AtABCC1*-reverse, 5′-ACCTTCCATTAATTTCAGCCATCC-3′; *AtABCC2*-forward, 5′-TTGATGCTGAGGTCTCTGAGG-3′, and *AtABCC2*-reverse, 5′-AGTATCTTAGATCTCCGTAACAGC-3′; *TUB1*-forward, 5′-ATGCTGATGAATGCATGGTCC-3′, and *TUB1*-reverse, 5′-TTCAAGTCTCCAAAGCTAGGAG-3′. Transcript levels were calculated using the standard curve method (Pfaffl et al., 2001) and normalized with *TUB1* (tubulin β-1 chain) expression levels.

Microarray Data Retrieval from the Genevestigator Database

Gene expression profiles of *AtABCC1*, *AtABCC2*, and *AtABCC14* were obtained from publicly available Affymetrix ATH1 microarray data provided by the Genevestigator database (http://www.genevestigator.com; Hruz et al., 2008). *AtABCC1* (Probeset identifier 256305_at) and *AtABCC2* (Probeset identifier 267319_at) expression levels in shoot tissues were obtained from experiments on drought stress and exogenous ABA application where the treatment duration was at least 4 h. Brief summaries and references of analyzed experiments are presented in Supplemental Table S1. *AtABCC14* (Probeset identifier 251227_at) expression values were obtained for the Development tool and from the following experiments on seed maturation and germination: AT-00116, AT-00117, AT-00490, AT-00509, and AT-00540. Figures were exported from Genevestigator and edited in Adobe Illustrator.

Information on genes referred to in this article can be found in the Arabidopsis Genome Initiative database (Lamesch et al., 2012) under the accession numbers At3g21780 (*AtUGT71B6*), At1g30400 (*AtABCC1*), At2g34660 (*AtABCC2*), At3g62700 (*AtABCC14*), and At1g75780 (*TUB1*).

Supplemental Data

The following materials are available in the online version of this article.

Supplemental Figure S1. Amount of synthesized ABA-GE dependent on the UDP-Glc amount used in the ABA-GE synthesis reaction.

Supplemental Figure S2. Absorption spectra from both synthesized and authentic ABA-GE measured during HPLC analysis.

Supplemental Figure S3. Elution profile of the ^{14}C radioactivity from a substrate mix separated on a HPLC system for the analysis of carbohydrates.

Supplemental Figure S4. Neutral red-stained isolated mesophyll vacuoles used in ABA-GE uptake assays.

Supplemental Figure S5. *AtABCC14* expression levels in seeds.

Supplemental Figure S6. *AtABCC14* expression levels during developmental stages.

Supplemental Figure S7. Time-dependent ABA-GE uptake of membrane vesicles from yeast expressing AtABCC14.

Supplemental Figure S8. Effects of ABA, ABA-GE, and the cytochrome P450 inhibitor tetcyclacis on *AtABCC1* and *AtABCC2* expression levels in Arabidopsis seedlings.

Supplemental Figure S9. Publicly available microarray data on *AtABCC1* and *AtABC2* expression levels from experiments on drought stress and exogenous ABA application.

Supplemental Table S1. Descriptions of data sets retrieved from Genevestigator that were used for Supplemental Figure S9.

Supplemental Data S1. Estimation of the in vivo ABA-GE uptake rate.

ACKNOWLEDGMENTS

We thank Marianne Suter-Grotemeyer and Prof. Doris Rentsch (University of Bern) and Maja Schellenberg, Rita Saraiva, Barbara Bassin, and Dr. Thomas Schneider (University of Zurich) for their excellent technical support and discussions. Furthermore, we thank Prof. Karl Kuchler (Medical University Vienna) for provision of the yeast strains and Dr. Won-Yong Song (Pohang University of Science and Technology) for providing the *AtABCC1/AtABCC2* knockout mutants and yeast expression constructs.

Received June 11, 2013; accepted September 9, 2013; published September 12, 2013.

LITERATURE CITED

Baier M, Gimmler H, Hartung W (1990) The permeability of the guard cell plasma membrane and tonoplast. J Exp Bot **41:** 351–358

Bauer H, Ache P, Lautner S, Fromm J, Hartung W, Al-Rasheid KAS, Sonnewald S, Sonnewald U, Kneitz S, Lachmann N, et al (2013) The stomatal response to reduced relative humidity requires guard cell-autonomous ABA synthesis. Curr Biol **23:** 53–57

Boursiac Y, Léran S, Corratgé-Faillie C, Gojon A, Krouk G, Lacombe B (2013) ABA transport and transporters. Trends Plant Sci **18:** 325–333

Boyer GL, Zeevaart JAD (1982) Isolation and quantitation of β-D-glucopyranosyl abscisate from leaves of *Xanthium* and spinach. Plant Physiol **70:** 227–231

Bray EA, Zeevaart JAD (1985) The compartmentation of abscisic acid and β-D-glucopyranosyl abscisate in mesophyll cells. Plant Physiol **79:** 719–722

Carter C, Pan S, Zouhar J, Avila EL, Girke T, Raikhel NV (2004) The vegetative vacuole proteome of *Arabidopsis thaliana* reveals predicted and unexpected proteins. Plant Cell **16:** 3285–3303

Chiwocha SDS, Abrams SR, Ambrose SJ, Cutler AJ, Loewen M, Ross ARS, Kermode AR (2003) A method for profiling classes of plant hormones and their metabolites using liquid chromatography-electrospray ionization tandem mass spectrometry: an analysis of hormone regulation of thermodormancy of lettuce (Lactuca sativa L.) seeds. Plant J **35:** 405–417

Christmann A, Weiler EW, Steudle E, Grill E (2007) A hydraulic signal in root-to-shoot signalling of water shortage. Plant J **52:** 167–174

Cutler SR, Rodriguez PL, Finkelstein RR, Abrams SR (2010) Abscisic acid: emergence of a core signaling network. Annu Rev Plant Biol **61:** 651–679

Dean JV, Mills JD (2004) Uptake of salicylic acid 2-O-β-D-glucose into soybean tonoplast vesicles by an ATP-binding cassette transporter-type mechanism. Physiol Plant **120:** 603–612

Dean JV, Mohammed LA, Fitzpatrick T (2005) The formation, vacuolar localization, and tonoplast transport of salicylic acid glucose conjugates in tobacco cell suspension cultures. Planta **221:** 287–296

Dietz KJ, Sauter A, Wichert K, Messdaghi D, Hartung W (2000) Extracellular β-glucosidase activity in barley involved in the hydrolysis of ABA glucose conjugate in leaves. J Exp Bot **51:** 937–944

Dröse S, Altendorf K (1997) Bafilomycins and concanamycins as inhibitors of V-ATPases and P-ATPases. J Exp Biol **200:** 1–8

Francisco RM, Regalado A, Ageorges A, Burla BJ, Bassin B, Eisenach C, Zarrouk O, Vialet S, Marlin T, Chaves MM, et al (2013) ABCC1, an ATP binding cassette protein from grape berry, transports anthocyanidin 3-*O*-glucosides. Plant Cell **25:** 1840–1854

Frangne N, Eggmann T, Koblischke C, Weissenböck G, Martinoia E, Klein M (2002) Flavone glucoside uptake into barley mesophyll and Arabidopsis cell culture vacuoles: energization occurs by H^+-antiport and ATP-binding cassette-type mechanisms. Plant Physiol **128:** 726–733

Frelet-Barrand A, Kolukisaoglu HÜ, Plaza S, Rüffer M, Azevedo L, Hörtensteiner S, Marinova K, Weder B, Schulz B, Klein M (2008) Comparative mutant analysis of Arabidopsis ABCC-type ABC transporters: AtMRP2 contributes to detoxification, vacuolar organic anion transport and chlorophyll degradation. Plant Cell Physiol **49:** 557–569

Galvan-Ampudia CS, Testerink C (2011) Salt stress signals shape the plant root. Curr Opin Plant Biol **14:** 296–302

Geisler M, Girin M, Brandt S, Vincenzetti V, Plaza S, Paris N, Kobae Y, Maeshima M, Billion K, Kolukisaoglu ÜH, et al (2004) Arabidopsis immunophilin-like TWD1 functionally interacts with vacuolar ABC transporters. Mol Biol Cell **15:** 3393–3405

Giaever G, Chu AM, Ni L, Connelly C, Riles L, Véronneau S, Dow S, Lucau-Danila A, Anderson K, André B, et al (2002) Functional profiling of the Saccharomyces cerevisiae genome. Nature **418:** 387–391

Gomez C, Terrier N, Torregrosa L, Vialet S, Fournier-Level A, Verriès C, Souquet JM, Mazauric JP, Klein M, Cheynier V, et al (2009) Grapevine MATE-type proteins act as vacuolar H^+-dependent acylated anthocyanin transporters. Plant Physiol **150:** 402–415

Goodger JQ, Schachtman DP (2010) Re-examining the role of ABA as the primary long-distance signal produced by water-stressed roots. Plant Signal Behav **5:** 1298–1301

Hocher V, Sotta B, Maldiney R, Miginiac E (1991) Changes in abscisic acid and its β-D-glucopyranosyl ester levels during tomato (Lycopersicon esculentum Mill.) seed development. Plant Cell Rep **10:** 444–447

Holdsworth MJ, Bentsink L, Soppe WJJ (2008) Molecular networks regulating Arabidopsis seed maturation, after-ripening, dormancy and germination. New Phytol **179:** 33–54

Hruz T, Laule O, Szabo G, Wessendorp F, Bleuler S, Oertle L, Widmayer P, Gruissem W, Zimmermann P (2008) Genevestigator v3: a reference expression database for the meta-analysis of transcriptomes. Adv Bioinforma **2008:** 420747

Huang D, Wu W, Abrams SR, Cutler AJ (2008) The relationship of drought-related gene expression in Arabidopsis thaliana to hormonal and environmental factors. J Exp Bot **59:** 2991–3007

Jaquinod M, Villiers F, Kieffer-Jaquinod S, Hugouvieux V, Bruley C, Garin J, Bourguignon J (2007) A proteomics dissection of Arabidopsis thaliana vacuoles isolated from cell culture. Mol Cell Proteomics **6:** 394–412

Kang J, Park J, Choi H, Burla B, Kretzschmar T, Lee Y, Martinoia E (2011) Plant ABC transporters. The Arabidopsis Book e0153

Kepka M, Benson CL, Gonugunta VK, Nelson KM, Christmann A, Grill E, Abrams SR (2011) Action of natural abscisic acid precursors and catabolites on abscisic acid receptor complexes. Plant Physiol **157:** 2108–2119

Kim TH, Böhmer M, Hu H, Nishimura N, Schroeder JI (2010) Guard cell signal transduction network: advances in understanding abscisic acid, CO_2, and Ca^{2+} signaling. Annu Rev Plant Biol **61:** 561–591

Klein M, Weissenböck G, Dufaud A, Gaillard C, Kreuz K, Martinoia E (1996) Different energization mechanisms drive the vacuolar uptake of a flavonoid glucoside and a herbicide glucoside. J Biol Chem **271:** 29666–29671

Kushiro T, Okamoto M, Nakabayashi K, Yamagishi K, Kitamura S, Asami T, Hirai N, Koshiba T, Kamiya Y, Nambara E (2004) The Arabidopsis cytochrome P450 CYP707A encodes ABA 8′-hydroxylases: key enzymes in ABA catabolism. EMBO J **23:** 1647–1656

Lamesch P, Berardini TZ, Li D, Swarbreck D, Wilks C, Sasidharan R, Muller R, Dreher K, Alexander DL, Garcia-Hernandez M, et al (2012) The Arabidopsis Information Resource (TAIR): improved gene annotation and new tools. Nucleic Acids Res **40:** D1202–D1210

Lazarowski ER, Shea DA, Boucher RC, Harden TK (2003) Release of cellular UDP-glucose as a potential extracellular signaling molecule. Mol Pharmacol **63:** 1190–1197

Lee KH, Piao HL, Kim HY, Choi SM, Jiang F, Hartung W, Hwang I, Kwak JM, Lee IJ, Hwang I (2006) Activation of glucosidase via stress-induced polymerization rapidly increases active pools of abscisic acid. Cell **126:** 1109–1120

Lehmann H, Glund K (1986) Abscisic acid metabolism: vacuolar/extravacuolar distribution of metabolites. Planta **168:** 559–562

Lim EK, Doucet CJ, Hou B, Jackson RG, Abrams SR, Bowles DJ (2005) Resolution of (+)-abscisic acid using an Arabidopsis glycosyltransferase. Tetrahedron Asymmetry **16:** 143–147

Lim PO, Kim HJ, Nam HG (2007) Leaf senescence. Annu Rev Plant Biol **58:** 115–136

Liu G, Sánchez-Fernández R, Li ZS, Rea PA (2001) Enhanced multispecificity of Arabidopsis vacuolar multidrug resistance-associated protein-type ATP-binding cassette transporter, AtMRP2. J Biol Chem **276:** 8648–8656

Lu YP, Li ZS, Drozdowicz YM, Hortensteiner S, Martinoia E, Rea PA (1998) AtMRP2, an *Arabidopsis* ATP binding cassette transporter able to transport glutathione *S*-conjugates and chlorophyll catabolites: functional comparisons with Atmrp1. Plant Cell **10:** 267–282

Lu YP, Li ZS, Rea PA (1997) AtMRP1 gene of Arabidopsis encodes a glutathione S-conjugate pump: isolation and functional definition of a plant ATP-binding cassette transporter gene. Proc Natl Acad Sci USA **94:** 8243–8248

Marinova K, Pourcel L, Weder B, Schwarz M, Barron D, Routaboul JM, Debeaujon I, Klein M (2007) The *Arabidopsis* MATE transporter TT12 acts as a vacuolar flavonoid/H^+-antiporter active in proanthocyanidin-accumulating cells of the seed coat. Plant Cell **19:** 2023–2038

Martinoia E, Grill E, Tommasini R, Kreuz K, Amrhein N (1993) ATP-dependent glutathione S-conjugate "export" pump in the vacuolar membrane of plants. Nature **364:** 247–249

Martinoia E, Kaiser G, Schramm MJ, Heber U (1987) Sugar transport across the plasmalemma and the tonoplast of barley mesophyll protoplasts: evidence for different transport systems. J Plant Physiol **131:** 467–478

Martinoia E, Meyer S, De Angeli A, Nagy R (2012) Vacuolar transporters in their physiological context. Annu Rev Plant Biol **63:** 183–213

Miao YC, Liu CJ (2010) ATP-binding cassette-like transporters are involved in the transport of lignin precursors across plasma and vacuolar membranes. Proc Natl Acad Sci USA **107:** 22728–22733

Nagy R, Grob H, Weder B, Green P, Klein M, Frelet-Barrand A, Schjoerring JK, Brearley C, Martinoia E (2009) The Arabidopsis ATP-binding cassette protein AtMRP5/AtABCC5 is a high affinity inositol hexakisphosphate transporter involved in guard cell signaling and phytate storage. J Biol Chem **284:** 33614–33622

Nambara E, Marion-Poll A (2005) Abscisic acid biosynthesis and catabolism. Annu Rev Plant Biol **56:** 165–185

Nilson SE, Assmann SM (2007) The control of transpiration: insights from Arabidopsis. Plant Physiol **143:** 19–27

Okamoto M, Kushiro T, Jikumaru Y, Abrams SR, Kamiya Y, Seki M, Nambara E (2011) ABA 9′-hydroxylation is catalyzed by CYP707A in Arabidopsis. Phytochemistry **72:** 717–722

Omote H, Hiasa M, Matsumoto T, Otsuka M, Moriyama Y (2006) The MATE proteins as fundamental transporters of metabolic and xenobiotic organic cations. Trends Pharmacol Sci **27:** 587–593

Park J, Song WY, Ko D, Eom Y, Hansen TH, Schiller M, Lee TG, Martinoia E, Lee Y (2012) The phytochelatin transporters AtABCC1 and AtABCC2 mediate tolerance to cadmium and mercury. Plant J **69:** 278–288

Paumi CM, Chuk M, Snider J, Stagljar I, Michaelis S (2009) ABC transporters in Saccharomyces cerevisiae and their interactors: new technology advances the biology of the ABCC (MRP) subfamily. Microbiol Mol Biol Rev **73:** 577–593

Payen L, Delugin L, Courtois A, Trinquart Y, Guillouzo A, Fardel O (2001) The sulphonylurea glibenclamide inhibits multidrug resistance protein (MRP1) activity in human lung cancer cells. Br J Pharmacol **132:** 778–784

Peters S, Mundree SG, Thomson JA, Farrant JM, Keller F (2007) Protection mechanisms in the resurrection plant Xerophyta viscosa (Baker): both sucrose and raffinose family oligosaccharides (RFOs) accumulate in leaves in response to water deficit. J Exp Bot **58:** 1947–1956

Pfaffl MW (2001) A new mathematical model for relative quantification in real-time RT-PCR. Nucleic Acids Res **29:** e45

Piotrowska A, Bajguz A (2011) Conjugates of abscisic acid, brassinosteroids, ethylene, gibberellins, and jasmonates. Phytochemistry **72:** 2097–2112

Priest DM, Jackson RG, Ashford DA, Abrams SR, Bowles DJ (2005) The use of abscisic acid analogues to analyse the substrate selectivity of UGT71B6, a UDP-glycosyltransferase of Arabidopsis thaliana. FEBS Lett **579:** 4454–4458

Rademacher W (2000) Growth retardants: effects on gibberellin biosynthesis and other metabolic pathways. Annu Rev Plant Physiol Plant Mol Biol **51:** 501–531

Raichaudhuri A, Peng M, Naponelli V, Chen S, Sánchez-Fernández R, Gu H, Gregory JF III, Hanson AD, Rea PA (2009) Plant vacuolar ATP-binding cassette transporters that translocate folates and antifolates in vitro and contribute to antifolate tolerance in vivo. J Biol Chem **284:** 8449–8460

Sauer N, Stolz J (1994) SUC1 and SUC2: two sucrose transporters from Arabidopsis thaliana: expression and characterization in baker's yeast and identification of the histidine-tagged protein. Plant J **6:** 67–77

Sauter A, Dietz K-J, Hartung W (2002) A possible stress physiological role of abscisic acid conjugates in root-to-shoot signalling. Plant Cell Environ **25:** 223–228

Seiler C, Harshavardhan VT, Rajesh K, Reddy PS, Strickert M, Rolletschek H, Scholz U, Wobus U, Sreenivasulu N (2011) ABA biosynthesis and degradation contributing to ABA homeostasis during barley seed development under control and terminal drought-stress conditions. J Exp Bot **62:** 2615–2632

Sharkey TD, Raschke K (1980) Effects of phaseic acid and dihydrophaseic acid on stomata and the photosynthetic apparatus. Plant Physiol **65:** 291–297

Shimaoka T, Ohnishi M, Sazuka T, Mitsuhashi N, Hara-Nishimura I, Shimazaki KI, Maeshima M, Yokota A, Tomizawa KI, Mimura T (2004) Isolation of intact vacuoles and proteomic analysis of tonoplast from suspension-cultured cells of Arabidopsis thaliana. Plant Cell Physiol **45:** 672–683

Sikorski RS, Hieter P (1989) A system of shuttle vectors and yeast host strains designed for efficient manipulation of DNA in Saccharomyces cerevisiae. Genetics **122:** 19–27

Song WY, Park J, Mendoza-Cózatl DG, Suter-Grotemeyer M, Shim D, Hörtensteiner S, Geisler M, Weder B, Rea PA, Rentsch D, et al (2010) Arsenic tolerance in Arabidopsis is mediated by two ABCC-type phytochelatin transporters. Proc Natl Acad Sci USA **107:** 21187–21192

Song WY, Sohn EJ, Martinoia E, Lee YJ, Yang YY, Jasinski M, Forestier C, Hwang I, Lee Y (2003) Engineering tolerance and accumulation of lead and cadmium in transgenic plants. Nat Biotechnol **21:** 914–919

The Arabidopsis Genome Initiative (2000) Analysis of the genome sequence of the flowering plant Arabidopsis thaliana. Nature **408:** 796–815

Tommasini R, Evers R, Vogt E, Mornet C, Zaman GJ, Schinkel AH, Borst P, Martinoia E (1996) The human multidrug resistance-associated protein functionally complements the yeast cadmium resistance factor 1. Proc Natl Acad Sci USA **93:** 6743–6748

Tossi V, Cassia R, Bruzzone S, Zocchi E, Lamattina L (2012) ABA says NO to UV-B: a universal response? Trends Plant Sci **17:** 510–517

Tsuyama T, Kawai R, Shitan N, Matoh T, Sugiyama J, Yoshinaga A, Takabe K, Fujita M, Yazaki K (2013) Proton-dependent coniferin transport, a common major transport event in differentiating xylem tissue of woody plants. Plant Physiol **162:** 918–926

van Zanden JJ, Wortelboer HM, Bijlsma S, Punt A, Usta M, Bladeren PJ, Rietjens IMCM, Cnubben NHP (2005) Quantitative structure activity relationship studies on the flavonoid mediated inhibition of multidrug resistance proteins 1 and 2. Biochem Pharmacol **69:** 699–708

Verslues PE, Agarwal M, Katiyar-Agarwal S, Zhu J, Zhu JK (2006) Methods and concepts in quantifying resistance to drought, salt and freezing, abiotic stresses that affect plant water status. Plant J **45:** 523–539

Wang P, Liu H, Hua H, Wang L, Song CP (2011) A vacuole localized β-glucosidase contributes to drought tolerance in Arabidopsis. Chin Sci Bull **56:** 3538–3546

Xu ZY, Kim DH, Hwang I (2013) ABA homeostasis and signaling involving multiple subcellular compartments and multiple receptors. Plant Cell Rep **32:** 807–813

Xu ZY, Lee KH, Dong T, Jeong JC, Jin JB, Kanno Y, Kim DH, Kim SY, Seo M, Bressan RA, et al (2012) A vacuolar β-glucosidase homolog that possesses glucose-conjugated abscisic acid hydrolyzing activity plays an important role in osmotic stress responses in *Arabidopsis*. Plant Cell **24:** 2184–2199

Zhao J, Dixon RA (2009) MATE transporters facilitate vacuolar uptake of epicatechin 3′-*O*-glucoside for proanthocyanidin biosynthesis in *Medicago truncatula* and *Arabidopsis*. Plant Cell **21:** 2323–2340

Zhao J, Huhman D, Shadle G, He XZ, Sumner LW, Tang Y, Dixon RA (2011) MATE2 mediates vacuolar sequestration of flavonoid glycosides and glycoside malonates in *Medicago truncatula*. Plant Cell **23:** 1536–1555